

 Open access • Proceedings Article • DOI:10.1063/1.1945008

## Systematic Analysis of Uranium Isotopes — [Source link](#)

[Phillip G. Young](#), [Mark B. Chadwick](#), [R. E. MacFarlane](#), [D. G. Madland](#) ...+4 more authors

**Published on:** 13 Jun 2005

**Topics:** [Isotopes of uranium](#), [Delayed neutron](#), [Neutron](#), [Uranium-235](#) and [Nuclide](#)

Related papers:

- [Evaluation of Neutron Reactions for ENDF/B-VII: 232–241U and 239Pu](#)
- [ENDF/B-VII.1 Nuclear Data for Science and Technology: Cross Sections, Covariances, Fission Product Yields and Decay Data](#)
- [EVALUATION AND TESTING OF n + 239pu DATA FOR ENDF/B-VI IN THE keV AND MeV ENERGY REGIONS](#)
- [New Nuclear Data Evaluations for Ca, Sc, Fe, Ge, Pb, and Bi Isotopes](#)
- [Status of the International Neutron Cross-Section Standards File](#)

Share this paper:    

View more about this paper here: <https://typeset.io/papers/systematic-analysis-of-uranium-isotopes-3002yp9to4>

LA-UR-04-0455

Approved for public release;  
distribution is unlimited.



Title: Systematic Analysis of Uranium Isotopes

Author(s): Phillip G. Young, Mark B. Chadwick, Robert E. MacFarlane,  
David G. Madland, Peter Moller, William B. Wilson, Patrick  
Talou, Toshihiko Kawano, T-16

Submitted to: Intl. Conf. on Nuclear Data for Science & Tech. ND2004  
Santa Fe, NM  
Sept. 26 - Oct. 1, 2004



Los Alamos National Laboratory, an affirmative action/equal opportunity employer, is operated by the University of California for the U.S. Department of Energy under contract W-7405-ENG-36. By acceptance of this article, the publisher recognizes that the U.S. Government retains a nonexclusive, royalty-free license to publish or reproduce the published form of this contribution, or to allow others to do so, for U.S. Government purposes. Los Alamos National Laboratory requests that the publisher identify this article as work performed under the auspices of the U.S. Department of Energy. Los Alamos National Laboratory strongly supports academic freedom and a researcher's right to publish; as an institution, however, the Laboratory does not endorse the viewpoint of a publication or guarantee its technical correctness.



# Systematic Analysis of Uranium Isotopes

Phillip G. Young, Mark B. Chadwick, Robert E. MacFarlane, David G. Madland,  
Peter Möller, William B. Wilson, Patrick Talou, and Toshihiko Kawano

*T-16, Nuclear Physics Group, Los Alamos National Laboratory*

**Abstract.** We describe recent Los Alamos nuclear model calculations and evaluations of neutron reactions on the uranium isotopes  $^{232-241}\text{U}$  in the keV - 30 MeV energy range. This work makes use of extensive sets of measurements for fission, elastic, inelastic, (n,xn) and capture, as well as fission probability data. The  $^{235}\text{U}(n,f)$  standard cross section was revised on the basis of improved experimental data, and the fission cross sections of the uranium isotopes, as well as  $^{237}\text{Np}$  and  $^{239}\text{Pu}$ , were updated using the revised standard. Nuclear reaction model calculations were performed for the whole suite of uranium isotopes to allow us to take advantage of the systematical properties from isotope-to-isotope, which is especially useful for nuclides where few measurements exist. In addition to improving the neutron cross sections and energy-angle distributions, new prompt fission neutron spectra and prompt/delayed neutron multiplicity evaluations are included for several isotopes.

## INTRODUCTION

We have carried out a program of systematic analysis of the nuclear reaction data on uranium isotopes from  $A = 232$  to  $241$ . New or revised evaluations of neutron data files for all the uranium isotopes have been completed covering the neutron energy range  $10^{-5}$  eV to 30 MeV. The evaluations are based on combinations of experimental data and theoretical model calculations. The isotopes with extensive experimental databases result in evaluations closely linked to measurements ( $^{233,235,238}\text{U}$ ). Several of the data files have looser links to experimental data ( $^{232, 234, 236}\text{U}$ ), and a few evaluations are based almost entirely on theoretical calculations and/or systematics ( $^{237,239,240,241}\text{U}$ ). Reports describing the  $^{233}\text{U}$ ,  $^{232,234}\text{U}$ , and the  $^{238}\text{U}$  evaluations have been published.<sup>1,2,3</sup>

Major features of this analysis include: systematic accumulation of all relevant experimental data; re-normalization of the neutron data to modern standards; assessment of the applicability of several recent optical model potentials for actinide calculations; interpretation of experimental results in terms of nuclear theory to allow interpolation and extrapolation of the data into unmeasured regions; and assemblage of the experimental and theoretical results into formal evaluated nuclear data files that can be processed for use in applied nuclear programs. In the course of the analysis, the standard  $^{235}\text{U}(n,f)$  cross section was updated for new experimental data and applied to all

the U-isotope evaluations, as well as to  $^{237}\text{Np}$  and  $^{239}\text{Pu}$  evaluations. All the work described here will be incorporated into Version VII of ENDF/B, with some revisions for Version VII standards, new experimental data, etc.

## THEORY AND MODELS

There were several objectives for our theoretical analysis. Firstly, we wished to provide a unified description of all reactions over the energy range 10 keV to 30 MeV for all uranium isotopes. Secondly, we needed consistent analyses of the measurement-rich systems in order to infer model parameters for the unmeasured systems. And thirdly, for all the isotopes we relied on the theoretical calculations for energy-angle correlated emission spectra, for elastic and inelastic neutron angular distributions, for (n,n'continuum) cross sections, and in most cases for (n,xn) cross sections. Our analysis consisted of developing suitable coupled-channels optical model potentials for each U isotope, and performing Hauser-Feshbach/statistical, preequilibrium, and direct reaction calculations.

We investigated several existing coupled-channels optical model potentials, which are based largely on  $^{238}\text{U}$  experimental data, in the uranium-isotope analysis. The potentials include (1) a new global

actinide potential developed by Vladuca *et al.*<sup>4</sup> that spans the incident neutron energy range from 1 keV to 20 MeV; (2) a new potential by Maslov *et al.*<sup>5</sup> covering the same energy range, developed by fitting s-wave strength functions and experimental neutron data; (3) an earlier potential (and variations) for  $E_n = 1$  keV to 30 MeV by Young and Arthur,<sup>6</sup> which was utilized for ENDF/B-VI evaluations; (4) a new  $^{238}\text{U} + n$  potential developed by Ignatyuk *et al.*<sup>7</sup> covering the energy range 1 keV – 150 MeV; (5) a new potential derived by Sukhovitskij *et al.*<sup>8</sup> by fitting  $^{238}\text{U} + n$  and  $^{238}\text{U} + p$  scattering angular distributions and neutron total cross sections up to 150 MeV; (6) an extensive modification<sup>9</sup> of the earlier  $^{238}\text{U} + n$  potential from Los Alamos<sup>6</sup> mentioned in item (3) above, covering the energy range out to 200 MeV; and, (7) a new potential by Maslov *et al.*<sup>10</sup> that covers the incident nucleon energy range from 1 keV to 200 MeV.

Optical model calculations were performed with the 1996 version of the ECIS coupled-channels optical model code by Raynal<sup>11</sup> to produce spin-dependent transmission coefficients for the Hauser-Feshbach calculations (below), as well as total and scattering cross sections to low-lying states. For most of the potentials, we coupled the lowest 3-7 ground-band rotational states into the calculations and included compound nucleus competition from uncoupled states plus a continuum of  $(n, n')$  states. The discrete levels were taken mainly from the International Atomic Energy Agency (IAEA) RIPL-2 database.<sup>12</sup> We also used ECIS96 for DWBA calculations to estimate contributions from  $\beta$ - and  $\gamma$ -vibrational states at various excitation energies between  $E_x = 0.5$  and 4 MeV, as described below.

Hauser-Feshbach statistical calculations were performed both with ECIS96 and with the GNASH statistical/preequilibrium theory code<sup>13</sup> using the same optical potentials and level density parameters. The GNASH code includes a double-humped fission barrier model using uncoupled oscillators for the barrier representation, as described by Arthur.<sup>14</sup> Each compound nucleus formed in the calculations is permitted to decay through the fission channel and by neutron and gamma-ray emission. Gamma-ray transmission coefficients are obtained from strength functions calculated with the generalized Lorentzian model of Kopecky and Uhl.<sup>15</sup> Transmission coefficients for fission are calculated from the fission model summarized here and detailed in ref. 13. Competition from fission was included in the ECIS96 compound nucleus calculations by appropriate scaling using the evaluated fission cross sections.

Continuous level density functions based on Fermi gas and constant temperature models<sup>16</sup> were used, with level density parameters chosen to reproduce s-wave level spacings,  $\langle D_0 \rangle$ , measured at the neutron separation energy.<sup>12</sup> Multiplicative factors are applied to the level density functions to account for enhancements in the fission transition state densities at the fission barriers due to increased asymmetry conditions, and the continuum level densities are combined with discrete fission transition states at each barrier. The discrete fission transition state spectra are calculated from bandhead information taken from calculations and compilations by Britt.<sup>17</sup>

A semiclassical exciton model is used to simulate preequilibrium particle emission. The matrix element normalization constant that describes the competition between precompound particle emission and internal transitions to higher exciton states in preequilibrium emission was typically fixed in the range 120-150 MeV<sup>3</sup>. Similarly, the nuclear single-particle state densities were typically set to  $A/13$  MeV<sup>-1</sup> in the asymptotic limit where shell effects are washed out. Gamma ray strength functions were normalized to experimental information<sup>12</sup> on  $2\pi\Gamma_\gamma/\langle D_0 \rangle$ , sometimes with a slight renormalization to optimize agreement of calculated  $(n, \gamma)$  cross sections with experimental data.

Initial values of fission barrier parameters were taken from the work of Britt,<sup>17</sup> which were then optimized by comparing calculated fission cross sections from GNASH with experimental data. In most cases fits to experimental fission cross sections were used directly in the evaluations. In our calculations of the  $(n, n'$ continuum),  $(n, 2n)$ ,  $(n, 3n)$ , and  $(n, 4n)$  reactions, we utilized Kalbach<sup>18</sup> angular distribution systematics to obtain correlated energy-angle distributions for the continuum reactions.

## EXPERIMENTAL DATA

There is a great deal of experimental data available for neutron-induced reactions on U isotopes, particularly for fission cross sections. We obtained all experimental data from either the EXFOR/CSISRS database at the National Nuclear Data Center at Brookhaven National Laboratory or the Nuclear Energy Agency in Paris.

Much of the fission cross-section data is relative to  $^{235}\text{U}$ . The cross section ratio measurements were converted to absolute values using a revision of the ENDF/B-VI  $^{235}\text{U}(n, f)$  standard cross section<sup>19</sup> made at Los Alamos by Talou and Young.<sup>20</sup> The ratios of the

Los Alamos  $^{235}\text{U}(n,f)$  and recent (preliminary) ENDF/B-VII standard cross sections to the ENDF/B-VI standard cross section are shown in Fig. 1.

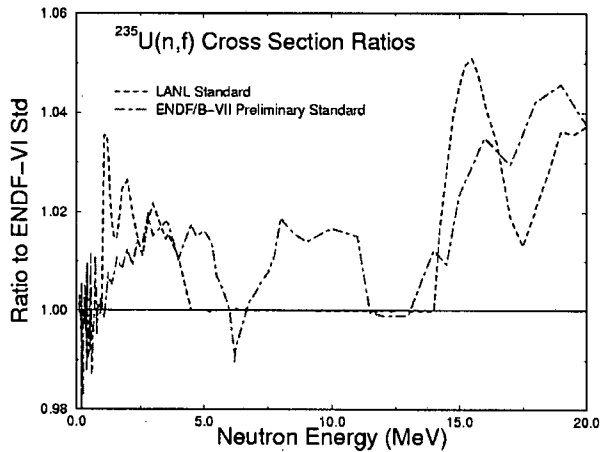


FIGURE 1. Ratios of LANL and preliminary ENDF/B-VII  $^{235}\text{U}(n,f)$  Cross Section Standards to ENDF/B-VI.

An important change occurs in the standard cross section in the 1-5 MeV region. This change is based on a combination of differential experimental data and fast critical integral experiments; and results in a decided improvement in simulations of the latter. Above 14 MeV, the Los Alamos reference cross section is taken from the International Atomic Energy Agency (IAEA) revised standard cross section<sup>21</sup> and is seen to be significantly higher than the ENDF/B-VI standard. The preliminary Version VII standard cross section was not available when our analysis was done.

Most of the prompt neutron multiplicities from fission ( $\bar{\nu}_p$ ) are also in the form of ratios, frequently relative to the very accurately known  $^{252}\text{Cf}$   $\bar{\nu}_p$  value. All prompt nubar measurements were adjusted to conform to ENDF/B-VI standards, where possible.

## EVALUATION FEATURES

### Total Cross Sections

We performed coupled-channels optical model calculations for all the uranium isotopes. In cases where experimental data were available ( $^{233,235,238}\text{U}$ ), the evaluated total cross sections are based on a combination of calculations and measurements. For  $^{235}\text{U}$  and  $^{238}\text{U}$ , results from a covariance analysis of the measurements were included in the analysis. For the remaining U isotopes, coupled channels optical calculations were used for the total cross sections.

Detailed assessments of the optical potentials<sup>1,3</sup> show that most of the potentials give reasonable results at most energies. For our evaluations, the Los Alamos optical model potentials<sup>1,6</sup> (or modifications thereof) were selected for our base coupled-channels calculations. In Fig. 2, the 1992 potential,<sup>6</sup> used for the  $^{238}\text{U}$  evaluation, is shown with the other potentials to agree reasonably with total cross section measurements. An overview of the evaluated total cross sections for the even-A isotopes is given in Fig. 3.

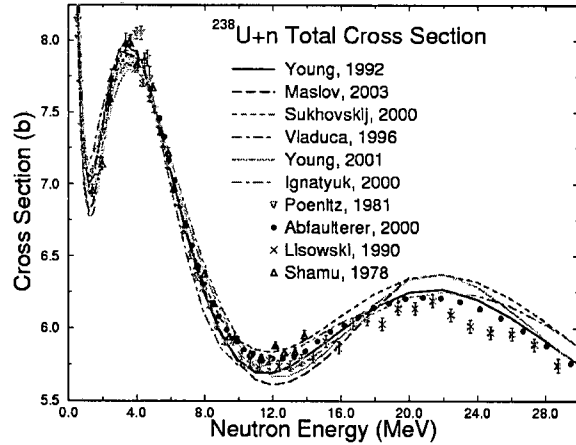


FIGURE 2. Comparison of Measured Total Cross Sections for  $^{238}\text{U}$  with Optical Model Calculations.

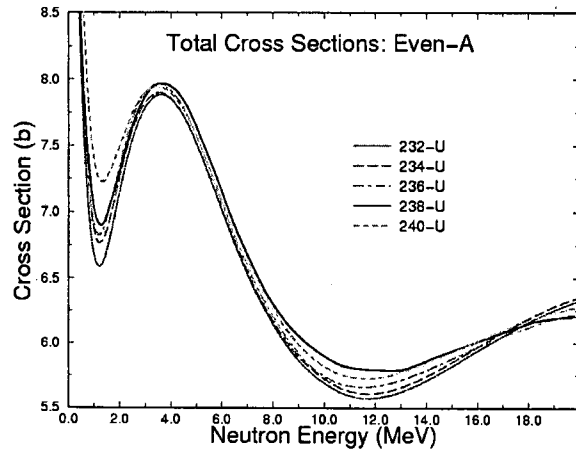


FIGURE 3. Evaluated Total Cross Sections for Even-A Uranium Isotopes.

### Fission Cross Sections and $\bar{\nu}_p$

Most of the uranium isotopes ( $^{232,233,234,235,236,238}\text{U}$ ) have useful experimental (n,f) cross section data for the evaluations. Two of the isotopes ( $^{237,239}\text{U}$ ) have fission probability data from (t,pf) surrogate reactions<sup>22</sup> that can be used in the evaluations.

GNASH reaction theory calculations were optimized to the experimental data, so that reliable calculations could be performed of the  $(n,n')$  and  $(n,xn)$  reaction channels. Fission barrier parameterizations were interpolated/extrapolated for GNASH calculations of the completely unmeasured target nuclei  $^{240,241}\text{U}$ .

The evaluated  $^{233}\text{U}(n,f)$  cross section between 2 and 16 MeV is compared to measurements in Fig. 4. In this case the GNASH calculation was utilized for the evaluation from 6-16 MeV. In Fig. 5, the GNASH calculation for the  $^{239}\text{U}(n,f)$  cross section is compared to experimental data inferred from surrogate measurements.<sup>22</sup> An overview of the evaluated  $(n,f)$  cross sections for the U isotopes is given in Fig. 6.

Prompt fission neutron multiplicities ( $\bar{\nu}_p$ ) were determined from experimental data on  $^{233,235,238}\text{U}+n$  reactions. For the remaining isotopes, previous evaluations and systematics were utilized.

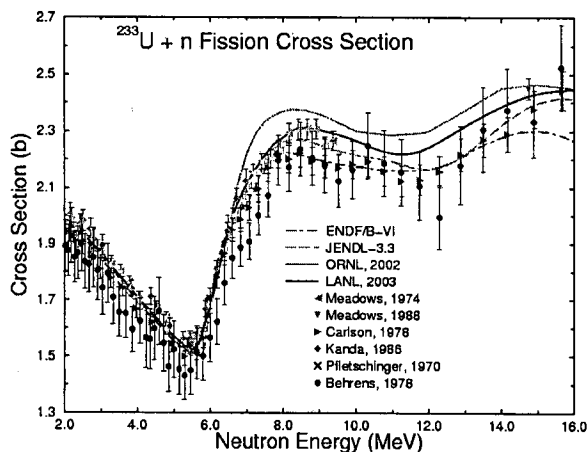


FIGURE 4. Evaluated and Measured  $^{233}\text{U}(n,f)$  Cross Sections.

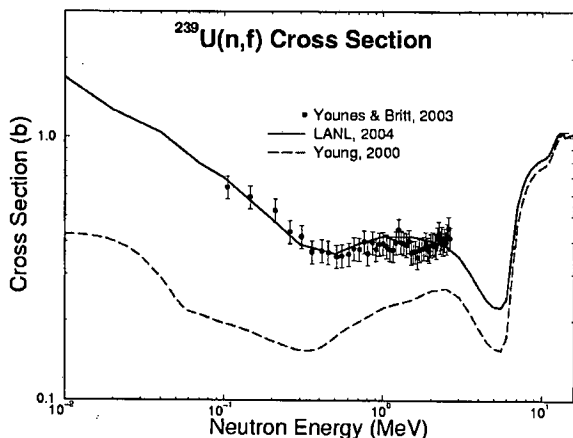


FIGURE 5. Calculated Surrogate  $^{239}\text{U}(n,f)$  Cross Sections.

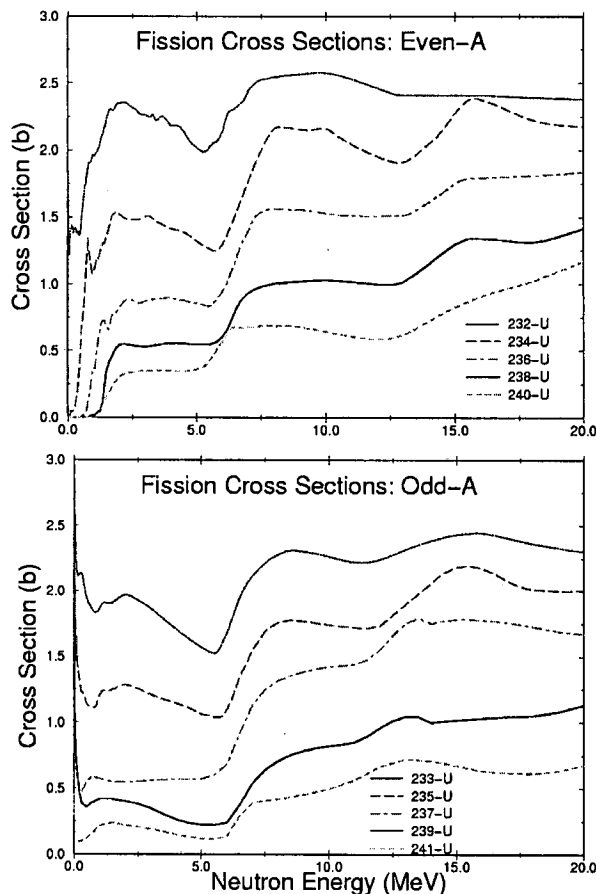


FIGURE 6. Evaluated U-Isotope Fission Cross Sections.

## Elastic & Inelastic Neutron Scattering

The evaluated elastic cross sections mainly result from coupled-channels optical calculations with the 1992 LANL potential,<sup>6</sup> although formally they were obtained by differencing the total and nonelastic cross sections. In most of the evaluations, we also utilize elastic angular distributions from the coupled-channels calculations. In the case of  $^{238}\text{U}$ , however, we discovered empirically that using angular distributions from the Maslov evaluation<sup>5</sup> below 10 MeV resulted in systematic improvement in calculations of several reactor benchmark experiments, so these were adopted. Neutron inelastic cross sections and angular distributions for discrete and continuum reactions were taken from the theoretical analyses, although several of the calculated  $^{238}\text{U}(n,n')$  cross sections were adjusted slightly to better match measurements. A comparison of measured and evaluated 2.5-MeV neutron elastic and inelastic ( $E_x=45$  keV) angular distributions for  $^{238}\text{U}$  is given in Fig. 7.

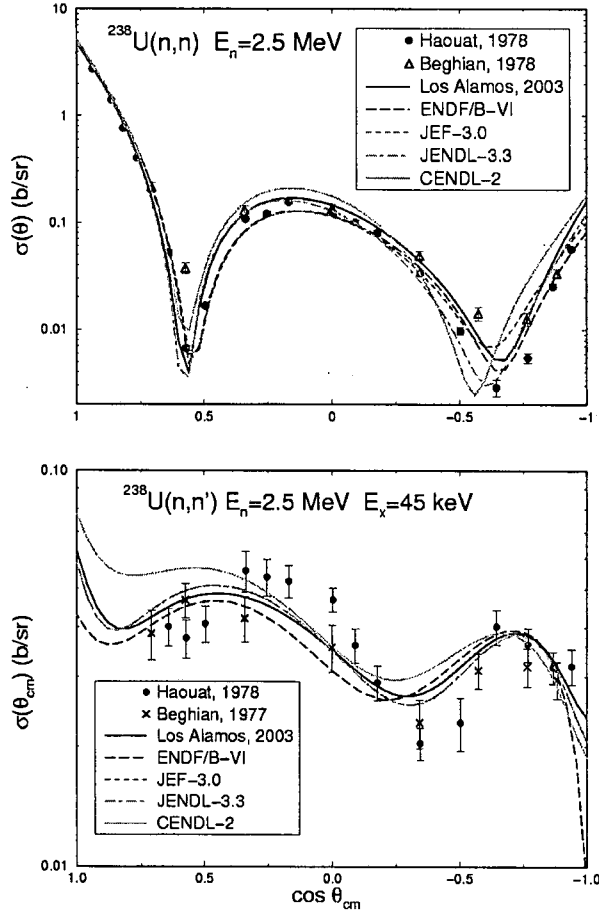


FIGURE 7. Evaluated and Measured  $^{238}\text{U}(n,n)$  and  $^{238}\text{U}(n,n')$  Angular Distributions for  $E_n=2.5$  MeV.

In both the  $^{235}\text{U}$  and  $^{238}\text{U}$  evaluations, we assume a set of  $J^\pi = 3^-$  and  $2^+$  states at excitation energies between  $E_x = 1-4$  MeV that are used to approximate unmeasured collective states. Similar to an earlier analysis of neutron emission spectra from  $^{184}\text{W}$  by Marcinkowski *et al.*,<sup>23</sup> it is not possible to account for the  $^{238}\text{U}$  neutron emission spectrum measurements of Baba *et al.*<sup>24</sup> at  $E_n = 14$  MeV by assuming only compound nucleus and preequilibrium reactions. We obtained cross sections and angular distributions for these states with DWBA calculations with ECIS96, with deformation parameters chosen to match Baba's 14-MeV data. These assumptions lead to significantly improved neutron emission spectra from  $^{238}\text{U}$  as well as to improved simulations of time-of-flight neutron distributions from pulsed-sphere experiments<sup>25</sup> in calculations with the MCNP Monte Carlo code.<sup>26</sup> Evaluated and measured double-differential spectra at  $E_n=11.8$  MeV ( $\theta=45^\circ$ ),  $E_n=14.05$  MeV ( $\theta=90^\circ$ ), and  $E_n=18.0$  MeV ( $\theta=120^\circ$ ) are compared in Fig. 8.

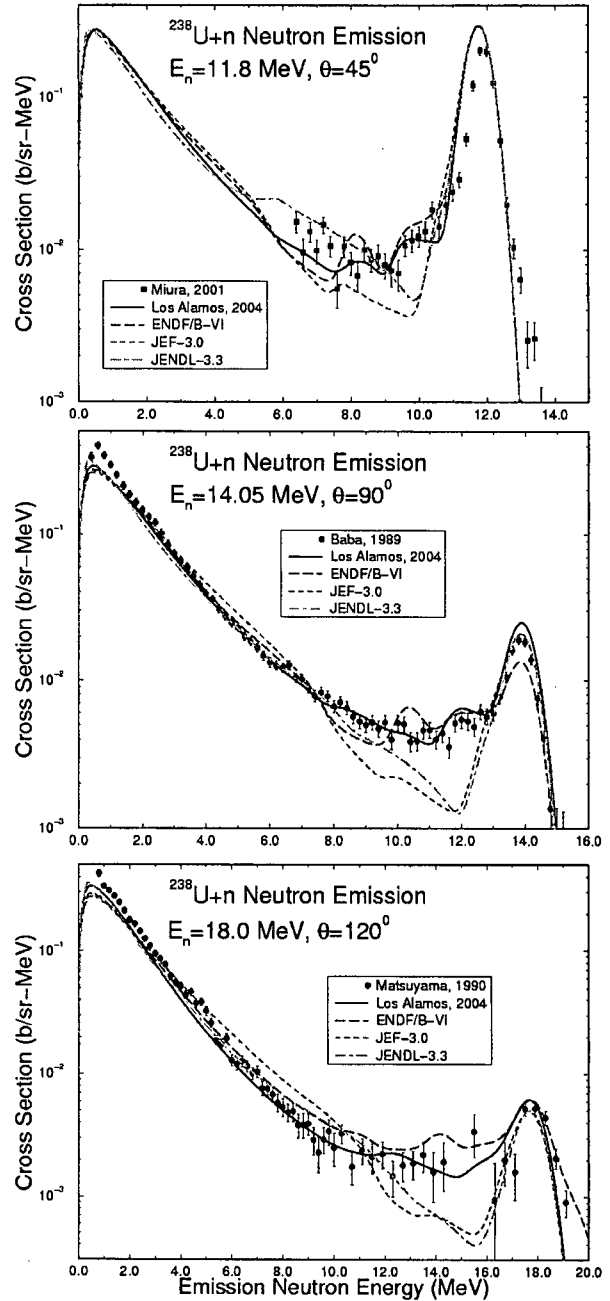


FIGURE 8. Double-Differential Neutron Emission Spectra from  $n+^{238}\text{U}$  Reactions Compared to Measurements.

### (n,xn) Cross Sections

Theoretical calculations played an important role in the  $(n,2n)$  and  $(n,3n)$  cross sections for all the uranium isotopes. The evaluated  $(n,2n)$  cross sections for  $^{235}\text{U}$  and  $^{238}\text{U}$  are compared to measurements in Fig. 9. The LANL  $^{235}\text{U}(n,2n)$  results are entirely from the GNASH calculation; the  $^{238}\text{U}(n,2n)$  evaluation is from GNASH at energies below 7.5 MeV and follows covariance

analysis results at higher energies. The behavior of the  $^{238}\text{U}$  cross section near threshold was validated in MCNP simulations<sup>27</sup> of critical assembly experiments having different degrees of hardness in their neutron spectra. The energy-angle neutron emission distributions from the GNASH analysis were used directly for all (n,xn) reactions, utilizing Kalbach<sup>18</sup> angular systematics.

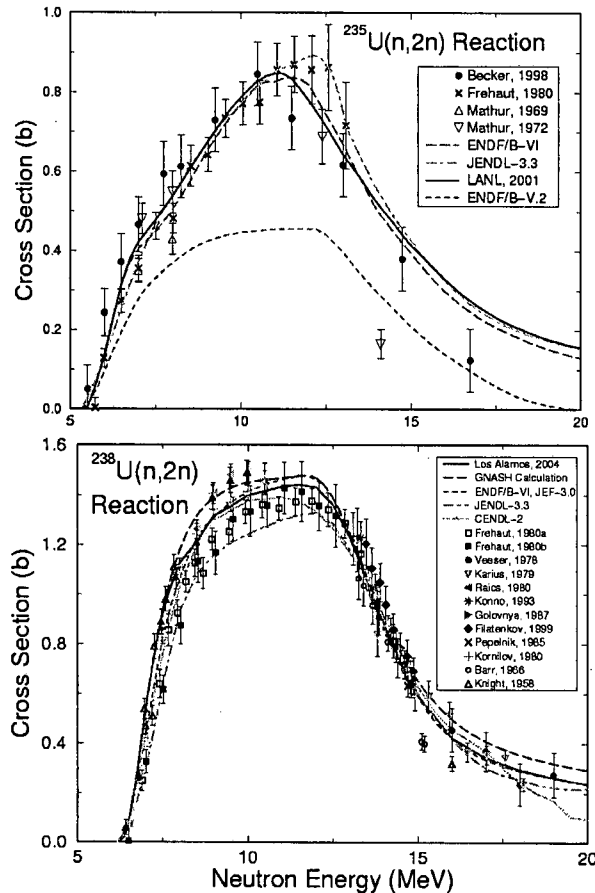


FIGURE 9. Evaluated and Measured (n,2n) Cross Sections for  $^{235}\text{U}$  and  $^{238}\text{U}$ .

## CLOSING REMARKS

We have completed new evaluations of neutron-induced reactions for 11 uranium isotopes over the incident neutron energy range  $10^5$  eV to 30 MeV. The new data files are part of the evaluation effort for Version VII of ENDF/B. Modifications will be made to the evaluations prior to release of ENDF/B-VII in order to incorporate final Version VII cross section standards and possibly other cross sections derived from the standards analysis. Other minor modifications based on recent measurements and

analyses may be incorporated, and inferences from data testing of the evaluations against integral experiments will also be considered.

## REFERENCES

1. Young, P. G, Chadwick, M. B., MacFarlane, R. E., Talou, P., LA-UR-03-1617 (2003)..
2. Young, P. G, et al., LA-UR-03-3205 (2003).
3. Young, P. G, et al., LA-UR, TBP (2004).
4. Vladuca, G., et al., *Rom. J. Phys.* **41**, 515 (1996).
5. Maslov, V. M., et al., INDC(BLR)-014 (2003).
6. Young, P. G., and Arthur, E. D. Jülich Conf., 13-17 May 1991 [ Springer-Verlag, Germany (1992)]
7. Ignatyuk, A V., Lunev, V. P., Shubin, Yu. N., Gai, E. V., et al., *Nucl. Sci. Eng.* **136**, 340 (2000).
8. Sukhovitskij, E. S., Iwamoto, O., Chiba, S., and Fukahori, T., *J. Nucl. Sci. & Tech.* **37**, 120 (2000).
9. Young, P. G., personal communication, 2001.
10. Maslov, V. M., et al., *Nucl. Phys.* **A736**, 1 (2004).
11. Raynal, J, CEA-N-2772 (1994).
12. "Handbook for Calculations of Nuclear Reaction Data: Reference Input Parameter Library, Version 2", to be issued as an IAEA-TECDOC (2004).
13. Young, P.G., Arthur, E.D., Chadwick, M.B., Proc. Wksp on *Nucl. Reaction Data and Nucl. Reactors*, ICTP, Trieste, Italy, 15 Apr -17 May 1996 [World Sci. Publ. Co., Singapore (1998)] p. 227-404.
14. Arthur, E. D, Proc. OECD/NEA Specialists' Mtg on *Fast Neutron Scattering on Actinide Nuclei*, (Paris, 1981), NEANDC-158 "U" (1982) p. 145.
15. Kopecky, J. et al., *Phys. Rev. C* **42**, 1941 (1990)
16. Gilbert, A. et al., *Can. J. Phys.* **43**, 1446 (1965).
17. Britt, H. C., personal communication, 1982.
18. Kalbach, C., *Phys. Rev. C* **37**, 2350 (1988).
19. Carlson, A. D. et al., NISTIR-5177 (May, 1993).
20. Talou, P., personal communication (2002).
21. Carlson, A. D. et al., INDC(NDS)-368 (1997).
22. Younes, W., Britt, H.C., UCRL-ID-154206 (2003)
23. Marcinkowski, A., Demetriou, P., Hodgson, P.E., *J. Phys. G [Nucl. & Part. Phys.]* **22**, 1219 (1996).
24. Baba, M., et al., JAERI-M-89-143 (1989).
25. Hansen, L. F., et al., *Nucl. Sci. Eng.* **72**, (1979).
26. Frankle, S., personal communication (2004); J. F. Briesmeister, ed., LA-13709-M (2000).
27. M. MacInnes, personal communication (2004).